Supplementary Figure legends

Figure 1 Echocardiographic analysis

Echocardiography was performed at indicated time points after TAC. **P<0.01. Data are represented as mean ± SEM; n=8-10. IVST, intraventricular septal thickness; FS, fractional shortening; LVDs, left ventricular end-systolic diameter.

Figure 2 Cardiac insulin signaling in the TAC heart at 1 week after operation

(**A**) Mice were subjected to TAC or sham operation (Sham), and heart samples were obtained 1 week later. Mice were starved for 6 hours, and insulin or PBS was injected before sacrifice. Phospho-IRS1 (pIrs1) and phospho-Akt (pAkt) levels in the heart were examined by Western blot analysis. The graphs indicate relative expression levels of pIrs1 and pAkt. *P<0.05, **P<0.01. Data are shown as the mean ± SEM; n=3.

(**B**) Mice were subjected to TAC or sham operation (Sham) and were sacrificed 1 week later. Components of the insulin signaling pathway in the heart were examined by Western blot analysis. The graphs indicate relative expression levels of these signaling molecules. *P<0.05, **P<0.01. Data are shown as the mean ± SEM; n=3.

(**C**) Mice were subjected to TAC or sham operation (Sham) and echocardiography was performed at 6 weeks after TAC. *P<0.05, **P<0.01. Data are shown as the mean ± SEM; n=3–5.

Figure 3 Up-regulation of cardiac insulin signals in spontaneously hypertensive rats (SHR)

(**A**) Eight-week-old Wistar-Kyoto rats (WKY) and spontaneously hypertensive rats (SHR) were starved for 6 hours, and insulin or PBS was injected before sacrifice. Phospho-Irs1 (pIrs1) and phospho-Akt (pAkt) levels in the heart were examined by Western blot analysis. The graphs indicate relative expression levels of pIrs1 and pAkt.

*P<0.05, **P<0.01. Data are shown as the mean ± SEM; n=3.

(**B**) Blood pressure measurement in Wistar-kyoto rats (WKY) and spontaneously hypertensive rats (SHR) at 8 weeks old. *P<0.05, **P<0.01. Data are shown as the mean ± SEM; n=4.

(**C**) Cardiac hypertrophy and systolic function were assessed by echocardiography at 8 weeks old. IVST, intraventricular septal thickness; FS, fractional shortening; LVDs, left ventricular end-systolic diameter. *P<0.05, **P<0.01. Data are shown as the mean ± SEM; n=3–5.

(**D**) Immunohistochemistry using antibodies against platelet and endothelial cell adhesion molecule (dark brown) and dystrophin (light brown) was performed at 8 weeks old. Scale bar, 20 μm. The cross-sectional area (CSA) of cardiomyocytes and relative vascular density were estimated as described in Methods. *P<0.05, **P<0.01. Data are shown as the mean ± SEM; n=3.

(**E**) Blood pressure measurement in Wistar-kyoto rats and spontaneously hypertensive rats (SHR) at 18 weeks old. *P<0.05, **P<0.01. Data are shown as the mean ± SEM; n=4.

(**F**) Cardiac hypertrophy and systolic function were assessed by echocardiography at 18 weeks old. IVST, intraventricular septal thickness; FS, fractional shortening; LVDs, left ventricular end-systolic diameter. *P<0.05, **P<0.01. Data are shown as the mean ± SEM; n=5.

(**G**) Immunohistochemistry double-stained with antibodies for platelet and endothelial cell adhesion molecule (dark brown) and dystrophin (light brown) was performed at 18 weeks old. Scale bar, 20 μm. The cross-sectional area (CSA) of cardiomyocytes and relative vascular density were estimated as described in Methods. *P<0.05, **P<0.01. Data are shown as the mean ± SEM; n=3.

Figure 4 Blood analysis

STZ- or vehicle-treated mice were subjected to TAC or sham operation (Sham). Plasma glucose and insulin levels were measured 2 weeks after operation. In the insulin-treated group, daily intraperitoneal injection of insulin (0.1 IU/g/day) was performed from 9 weeks (2 weeks after STZ treatment) to 13 weeks of age (2 weeks after TAC). **P<0.01. Data are represented as mean ± SEM; n=5.

Figure 5 Effect of COMP-Ang1 on cardiac dysfunction under chronic pressure overload

(**A**) Insulin-treated diabetic mice were subjected to TAC operation and simultaneously treated with adenoviral vector encoding COMP-Ang1 or LacZ. Immunohistochemistry using antibodies against platelet and endothelial cell adhesion molecule (dark brown) and dystrophin (light brown) was performed at 2 weeks after operation. Scale bar, 20 μm. The cross-sectional area (CSA) of cardiomyocytes and relative vascular density were estimated as described in Methods. *P<0.05, **P<0.01. Data are shown as the mean ± SEM; n=3.

(**B**) Cardiac ischemia (brown) in mice prepared according to the legend for Supplemental Figure 5A was estimated with a Hypoxyprobe 2 weeks after operation. Scale bar, 1 mm.

(**C**) Cardiac hypertrophy and systolic function were assessed by echocardiography 2 weeks after operation. FS, fractional shortening; LVDs, left ventricular end-systolic diameter. *P<0.05, **P<0.01. Data are shown as the mean ± SEM; n=3-5.

Figure 6 Echocardiography of CIRKO mice at 6 weeks after TAC operation

CIRKO mice (*Insr*$^{flox/+}$ Cre^{+}) or littermate controls (Control) were subjected to TAC or sham operation (Sham). Cardiac hypertrophy and systolic function was assessed by echocardiography 6 weeks after TAC. FS, fractional shortening; LVDs, left ventricular

end-systolic diameter. *P<0.05, **P<0.01. Data are shown as the mean ± SEM; n=3.

Figure 7 Acute pressure overload in heterozygous CIRKO mice

CIRKO mice (*Insr*$^{flox/+}$ Cre^{+}) were subjected to TAC or sham operation (Sham), and heart samples were obtained at the indicated times. Phospho-Irs1 (pIrs1) levels were examined by Western blot analysis. The graphs indicate relative expression levels of pIrs1. *P<0.05, **P<0.01. Data are shown as the mean ± SEM; n=3.

Figure 8 Involvement of insulin-like growth factor 1 and its receptor

Small-interfering RNA targeting insulin-like growth factor 1 (Igf1) or the Igf1 receptor (Igf1r) was introduced into cardiomyocytes, after which the cells were subjected to mechanical stretch. Phospho-Irs1 (pIrs1) levels were examined by Western blot analysis. The graphs indicate relative expression levels of pIrs1. *P<0.05, **P<0.01. Data are shown as the mean ± SEM; n=3.

Supplemental Figure 1

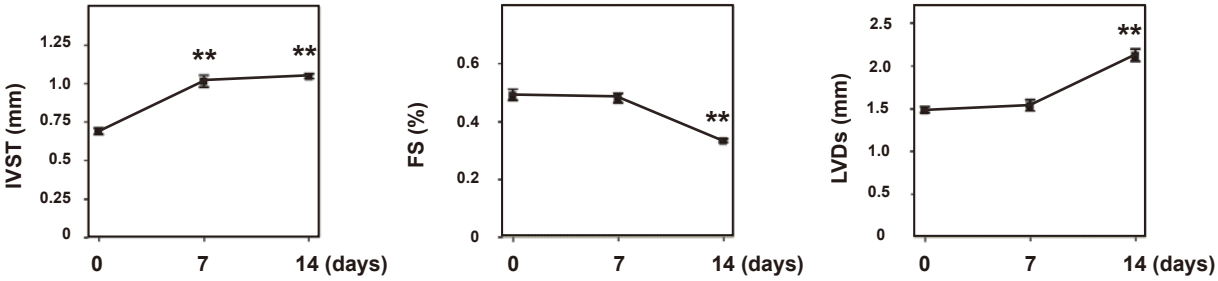

Supplemental Figure 2

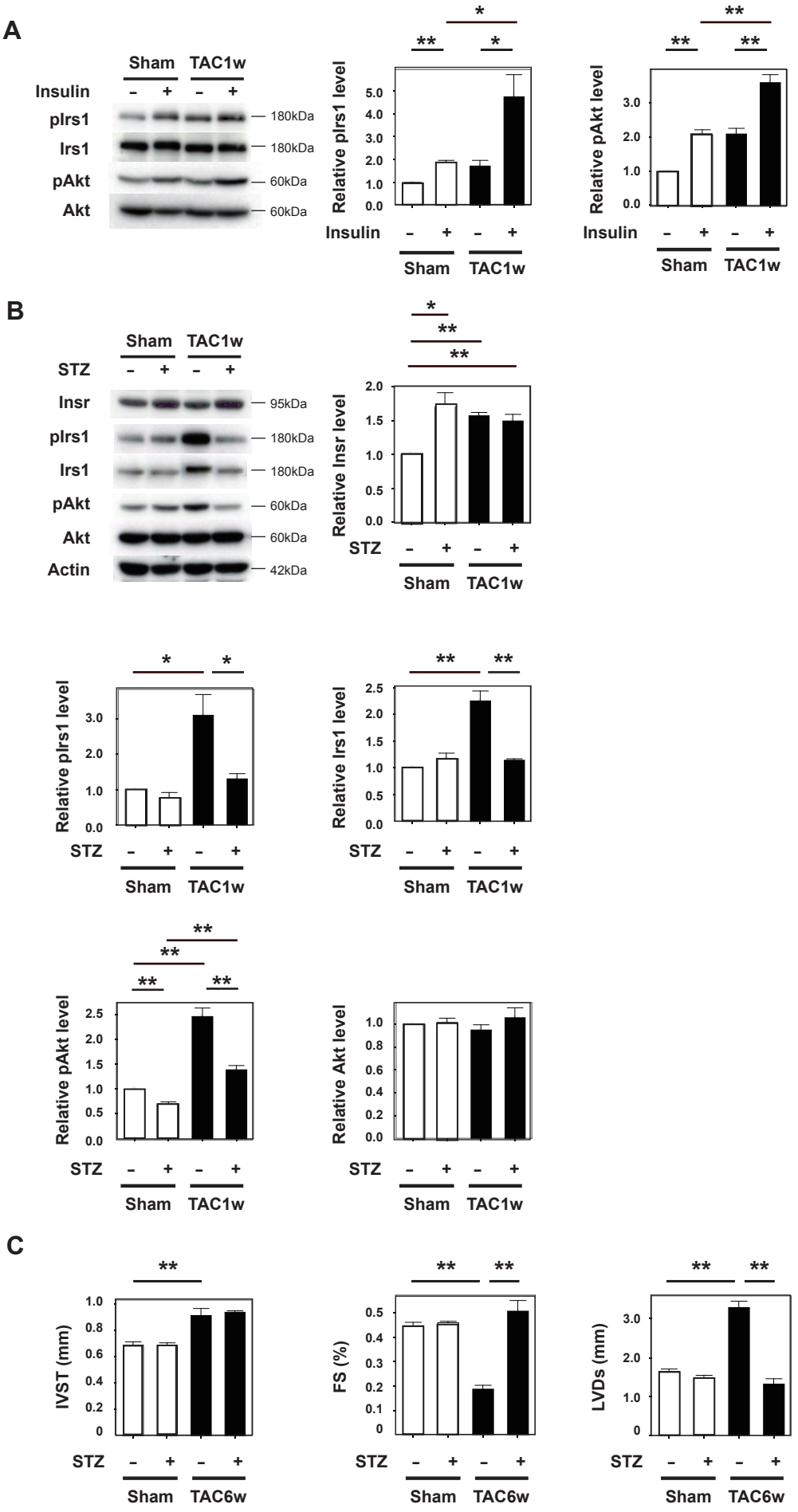

Supplemental Figure 3

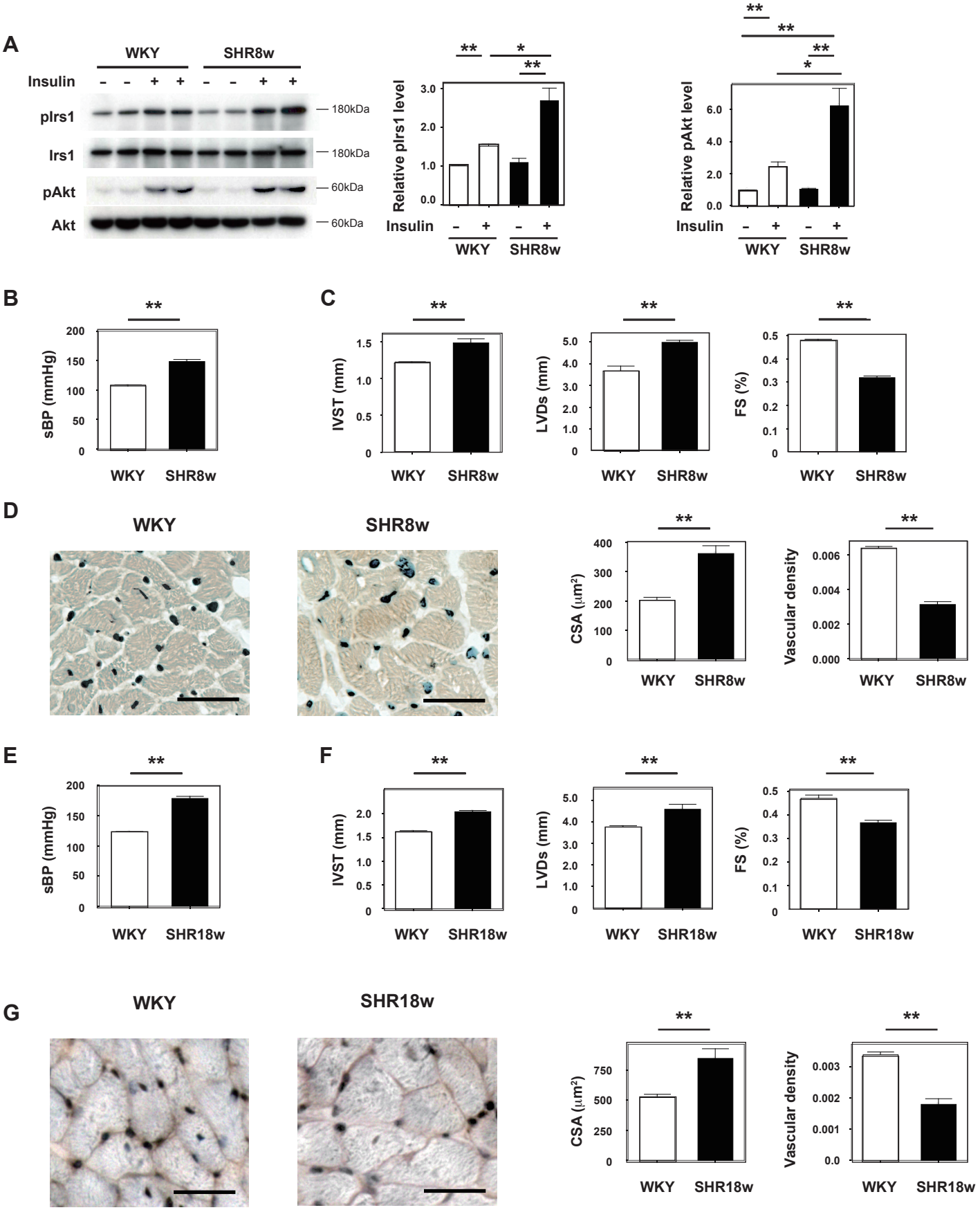

Supplemental Figure 4

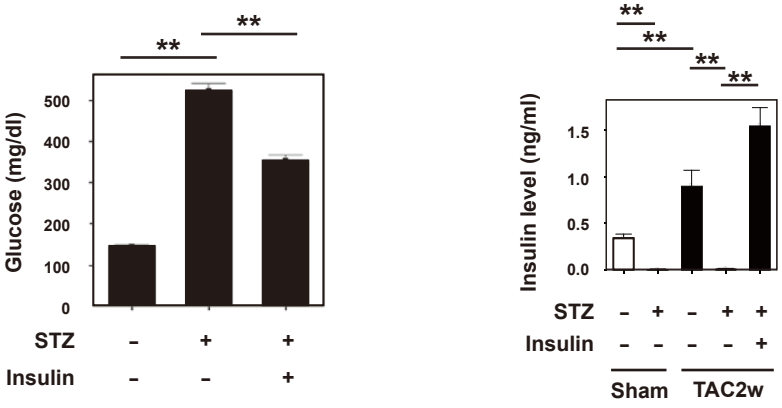

Supplemental Figure 5

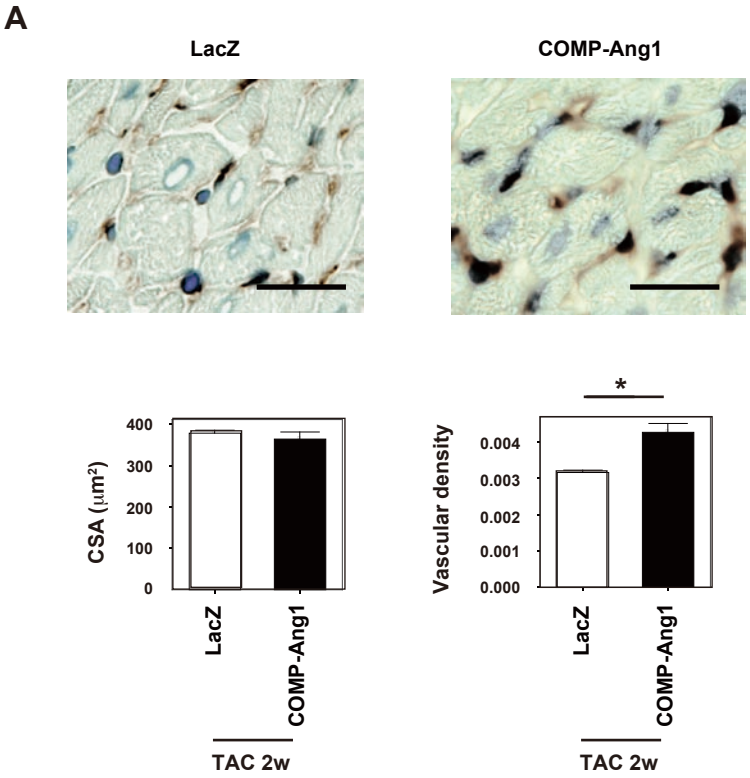

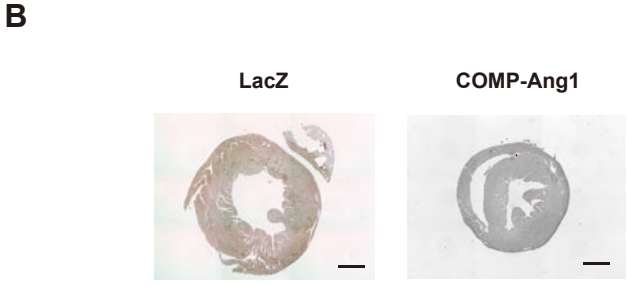

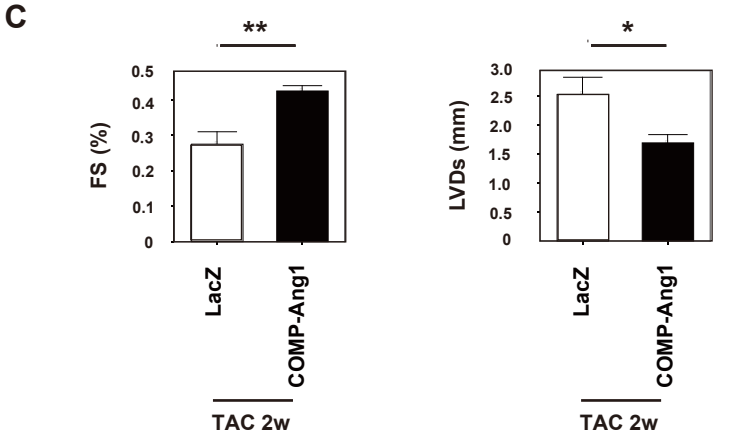

Supplemental Figure 6

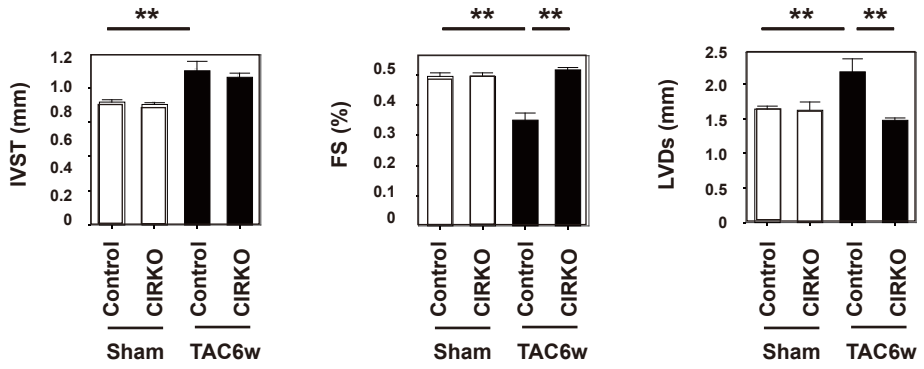

Supplemental Figure 7

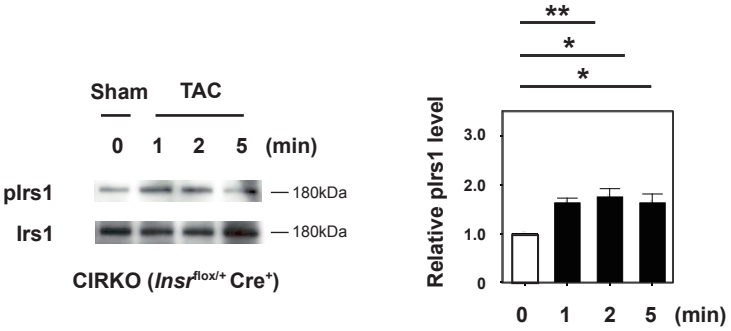

Supplemental Figure 8